Intestinal rotation and physiological umbilical herniation during the embryonic period

[1]Yui Ueda, [1,2]Shigehito Yamada, [2]Chigako Uwabe, [3]Katsumi Kose, [1]Tetsuya Takakuwa

1) Human Health Science, Graduate School of Medicine, Kyoto University, Sakyo-ku Shogoin Kawahara-cho 53, Kyoto, 606-8507, Japan
2) Congenital Anomaly Research Center, Graduate School of Medicine, Kyoto University, Sakyo-ku Yoshida-Konoe-cho Kyoto, 606-8501, Japan
3) Institute of Applied Physics, University of Tsukuba, Tenoudai 1-1-1, Tsukuba, Ibaragi, 305-8573, Japan

Corresponding author: Dr. Tetsuya Takakuwa
Human Health Science, Graduate School of Medicine, Kyoto University
606-8507 Sakyo-ku Shogoin Kawahara-cho 53, Kyoto, Japan
E-mail: tez@hs.med.kyoto-u.ac.jp; TEL: +81-75-751-3931

Running title: Intestinal rotation of human embryo

Grant Support
This study was supported by grants from the Japan Society for the Promotion of Science and the BIRD of Japan Science and Technology Agency (JST); Grant

number: #24119002, #25461642, #26220004, #15H01119, #15K15014,
#15K08134, #15H05270, #15H01121

Abstract

Drastic changes occur during the formation of the intestinal loop (IL), including elongation, physiological umbilical herniation (PUH), and midgut rotation. Fifty-four sets of magnetic resonance images of embryos between Carnegie stage (CS) 14 and CS 23 were used to reconstruct embryonic digestive tract in three dimensions in the Amira program. Elongation, PUH, and rotation were quantified in relation to the proximal part of the superior mesenteric artery (SMA), designated as the origin. Up to CS 16, IL rotation was initially observed as a slight deviation of the duodenum and colorectum from the median plane. The PUH was noticeable after CS 17. At CS 18, the IL showed a hairpin-like structure, with the SMA running parallel to the straight part and the cecum located to the left. After CS 19, the IL began to form a complex structure as a result of the rapid growth of the small intestinal portion. By CS 20, the IL starting point had moved from the right cranial region to an area caudal to the origin, though elongation of the duodenum was not conspicuous—this was a change of almost 180° in position. The end of the IL remained in roughly the same place, to the left of and caudal to the origin. Notably, the IL rotated around the origin only during earlier stages and gradually moved away, running transversely after CS 19. The movements of the IL may be explained as the result of differential growth, suggesting that IL rotation is passive.

Key Words

human embryo, intestinal development, midgut rotation, magnetic resonance imaging, three-dimensional reconstruction

Abbreviation

superior mesenteric artery (SMA), intestinal loop (IL), OE; omphalo-enteric duct, magnetic resonance (MR), Carnegie stage (CS), Three-dimensional (3D), Starting point of IL (S), Ending point of IL (E), Crown-Ramp length (CRL) point near the pyloric antrum (P), starting of IL (S), ending of IL, (E), cecum (C), tip of the IL (T), point crossing the border between abdominal coelom and extraembryonic coelom in the umbilical cord on the colon (B), omphalo-enteric duct (OE), angle between median plane and segment SE was calculated (∠Ro)

Introduction

The intestine elongates considerably during the embryonic period, and this involves two important phenomena, physiological umbilical herniation (PUH) (Meckel, 1817) and rotation (Mall, 1898). Those phenomena occur simultaneously and affect each other, making the process complicated to describe. Briefly, in PUH, the elongated intestine temporarily enters the extraembryonic coelom in the umbilical cord, rotating through 90° in a counterclockwise direction. This is followed by reduction, in which the intestine returns to the abdominal coelom, rotating a further 90° counterclockwise. In the final phase, fixation, the intestine assumes its final position as the mesentery rotates through 90°, again counterclockwise. The timing of PUH (Frazer and Robbins, 1915; O'Rahilly and Muller, 2001; Cyr et al., 1986) and the speed and timing of reduction (Mall, 1898; Cyr et al., 1986, Snyder and Chaffin, 1952, 1954) were subjects of debate until Kim et al. (2003), using histological analysis, found that initiation of the intestinal loop (IL) occurs at Carnegie stage (CS) 14, with PUH beginning around CS 16 and reaching its maximum at CS 23. The IL returns to the abdominal coelom when the crown-rump length (CRL) of the fetus is around 40 mm. However, the timing and degree of rotation are still being argued (Frazer and Robbins, 1915; Dott, 1922). In fact, Kluth et al. (1995, 2003, 2011) claim that there is no conclusive evidence for the rotation of the gut, because a malrotated gut has never been observed in normal embryos. On the basis of a scanning electron microscope study of IL formation in a rat model, they emphasize the importance of the formation of the duodenal loop and state that malformations are exclusively the result of localized growth failures of this

loop. They also deny that the cecum moves to the right lower part of the abdomen during fixation. Soffers et al. (2015) have developed hierarchical models based on 3D reconstruction of the midgut, superior mesenteric artery (SMA), and mesentery as a whole from histological sections; their models also differ from the classical en bloc rotation model.

Analysis and understanding of embryological intestinal development is undoubtedly important, as failure of the process can give rise to malformations such as nonrotation, malrotation, and subhepatic cecum. There is a need for quantitative, stage-by-stage descriptions of the process, based on three-dimensional (3D) images. The present study was designed to document and measure the movements of the intestine during elongation, PUH, and rotation in three dimensions; this was done using magnetic resonance (MR) microscopy to obtain images of embryos between CS 14 and CS 23, corresponding to the period from the initiation of the IL to maximum PUH.

Materials and Methods

Human embryo specimens

Approximately 44,000 human embryos, comprising the Kyoto Collection of Human Embryos, are stored at the Congenital Anomaly Research Center of Kyoto University (Nishimura et al., 1968; Shiota et al., 2007; Yamada et al., 2006). Most of these were obtained after termination of a pregnancy during the first trimester for socioeconomic reasons under the Maternity Protection Law of Japan. In the laboratory, aborted embryos were measured, examined, and

staged by two of the authors (C. U. and S. Y.) using the criteria provided by O'Rahilly and Müller (1987). Approximately 1,200 well-preserved embryos, found to be normal on gross examination and between CS 14 and CS 23, were selected for MR microscopy using methods previously described elsewhere (Shiota et al., 2007; Yamada et al., 2006; Matsuda et al., 2003, 2007). Of the 1,200 resulting MR image sets, the authors selected 54 displaying an intact umbilicus and body area for analysis of dimensional changes (3–7 for each CS).

Image analysis

The structure of the digestive tract, including the stomach, duodenum, IL, and colorectum, was reconstructed for each image set using the Amira software suite (version 5.4.5; Visage Imaging, Berlin, Germany) (Fig. 1a). The AmiraSkel software module was used to determine the centerline length of the digestive tract.

Anatomical landmarks and position of the intestine

The 3D coordinates were initially assigned by using Amira to examine the positions of particular voxels in 3D images. Two points on the proximal straight part of the SMA were designated Z1 and Z2 and used as external anatomical landmarks, and the line connecting the points was defined as the z-axis of the coordinate system (Fig. 1a,b). Point P, located on the digestive tract near the pyloric antrum above the neural tube and vertebral column, was used to determine the median plane and y-axis (Fig. 1b) (Kaigai et al., 2014). Various other points on the tract were used as internal anatomical landmarks, including

130 the start of the IL (S), the end of the IL (E), the cecum (C), the tip of the IL (T),
131 and point B, located where the border between the abdominal coelom and
132 extraembryonic coelom (specifically the umbilical cord) crossed the straight part
133 of the colonic portion of the IL. S and E were defined as the most obvious dorsal
134 inflection points on the 3D image and may correspond to the points at which the
135 length of the mesentery drastically changed as described by Soffers et al.
136 (2015).
137 The lengths of the duodenum (segment PS), small intestinal part of the IL
138 (segment SC), and large intestinal part of the IL (segment CE) were measured.
139 The distance from E to the rectum was not measured because it was difficult to
140 precisely locate the colorectum within the pelvic cavity using our methods. The
141 heights of T, B, and C were measured to estimate the extent of PUH (Fig. 1c).
142 Point T corresponded to the entry of the omphaloenteric duct, which could
143 occasionally be visualized. The z-coordinate of each landmark was recorded as
144 its height. CRL and maximal abdominal transverse length were used as
145 references for embryonic axial growth and width, respectively. To estimate the
146 position and rotation of the IL at points S and E, the angle between the median
147 plane and segment SE was calculated (angle of rotation, ∠Ro). The angles
148 formed with the median plane by points S and E were measured as ∠s and ∠e,
149 respectively, and the length of segment SE was also measured (Fig.1d).
150 The ethics committee of the Kyoto University Graduate School and Faculty of
151 Medicine approved this study (E986).
152

Results

Morphological changes of the intestinal tract during the embryonic period

The 3D anatomy of the intestinal tract was reconstructed using Amira (Fig. 2). The IL's development of a complex coiled, spiral structure during development was successfully visualized. Elevation of the intestinal tract was already observable at CS 14 (Fig. 2a), though points S and E were not clearly defined. From CS 16 onward, points S and E and the cecum were clearly recognizable. At CS 16, point T was located near the border between the abdominal coelom and extraembryonic coelom. The border area was broad and tilted caudad, making it difficult to determine whether the tip of the intestine had entered the umbilical cord or not. Both the duodenum and colorectum ran parallel to the median plane, with the duodenum shifted slightly to the right and the colorectum shifted slightly to the left. The IL connected both parts obliquely like a bridge. Viewed ventrally, the tract formed a crank shape (Fig. 2a).

At CS 17, PUH of the intestine, including the cecum, was evident (data not shown). By CS 18, the intestine had elongated and formed a straight tube like a hairpin (Fig. 2b). The SMA ran straight, parallel and proximate to both the efferent and afferent parts of the IL. The efferent part was on the right of the SMA, and the afferent part was on the left. The cecum and vermiform appendix could be distinguished to the left of the SMA in the umbilicus.

From CS 19 onward, the small intestinal portion of the IL began to show marked elongation and coiling, whereas the large intestinal portion remained almost straight until CS 23 (Fig. 2c). At these later stages, point E was located near the left gonadal ridge and metanephros, which were caudal to the origin

(data not shown).

Dimensional changes of the intestinal tract from CS 14 to CS 23

Elongation of the intestinal tract

The lengths of each previously mentioned segment of the intestinal tract were measured. CRL, the indicator of embryonic axial growth, increased nearly 3.6 times greater at CS 23 than at CS 16 (Fig. 3). The intestinal tract elongated rapidly over this period, primarily owing to the growth of segment SC (the small intestinal part of the IL). As a result, looping, coiling, and spiral formation were observed, first in the umbilicus and later inside the abdominal coelom. The lengths of the duodenum and the large intestinal part of the IL increased gradually over time. Compared with CS 16, the small intestinal part of the IL was 20 times longer by CS 23, whereas the large intestinal part was 8 times longer and the duodenum only 3.5 times longer.

Physiological umbilical herniation of the intestinal tract

The heights of the point of PUH and the border of the abdominal coelom increased gradually, at a rate similar to the increase in CRL (Fig. 4). The height ratios between T and B and between C and B were almost constant between CS 17 and CS 23 (T to B, 1.79–2.13; C to B, 1.10–1.38). The cecum could consistently be located at the proximal part of the umbilical cord, implying that the main part of the colorectum remained inside the abdominal coelom.

Movements of the intestinal tract

Points S and E were plotted on the coordinates with the proximal part of the SMA as the origin (Fig. 5a). As CS stage advanced, Point S moved caudally from the right cranial region of the SMA (in the second quadrant) to a point just right of the SMA, finally settling caudad of origin, almost in the median plane. Point E started out left of and caudal to the SMA (in the fourth quadrant) and gradually moved caudad. The distance between points S and E remained almost constant between CS16 and CS23 (715–1330 μm on the xy plane). The maximum abdominal transverse length increased gradually from 2.43 mm at CS 16 to 6.24 mm at CS 23.

Viewed ventrally, the IL was slightly tilted toward the median plane (Fig. 2a) at angle of 16.7° at CS 14 and 34.5° at CS 15. Though points S and C were clearly identifiable after CS 16, the angle between segment SE and the median plane (∠Ro), which was 43.6° at CS 16, reached near perpendicularity (92.3°) at CS 19 (Fig. 6). Notably, segment SE was rotated around the SMA only during earlier stages (up to CS 17); after CS 18, it moved caudad from the origin (Fig. 5a).

The movements of points S and E relative to the SMA were measured by their angles to the median plane. From CS 16 to CS 17, ∠s increased from 59.9° to 106.8°; by CS 23, it was 184.1°. In contrast, ∠e remained almost constant from CS16 to CS23 (changing from 25.5° and 44.6°).

The cecum was consistently located to the left of the SMA, generally at a distance of 500 to 1000 μm, though position varied as development proceeded (Fig. 5b).

Discussion

In the present study, we used 3D reconstruction to observe the dimensional changes of the intestinal tract between CS 14 and CS 23, corresponding to the period from the formation of the IL to PUH. Our observations were consistent with previous reports of the timeline of development (Kim et al., 2003), with the IL already observable at CS 14. PUH started at CS 16 and was noticeable by CS 17, with the extent of PUH increasing until CS 23.

Regarding rotation, there were several notable findings. The intestinal tract initially ran in the median plane, which was connected with the mesentery (Snyder and Chaffin, 1954). The transverse distance between the duodenum and colorectum changed slightly but significantly from CS 14 to CS 16, which formed a crank shape in ventral view with points S and E as vertices (Figs. 2a, 7a). Though the mechanism by which this laterality might happen is not yet known, it may be related to the developing liver and left umbilical vein (Frazer and Robbins, 1915) or to the helical body axis and descent of the upper abdominal structure (Soffers et al., 2015). The discrepancies in the literature regarding the timing of rotation initiation may result from this small but important phenomenon being overlooked or not regarded as part of rotation. Kim et al.

(2003) and Mall (1898) indicate that rotation begins at CS 15, just before the IL enters the umbilical cord. Other authors place the initiation of PUH and that of rotation at same time, around CS 16 or 17 (Frazer and Robbins, 1915).

We observed the origin (the proximal part of the SMA) to be located along segment SE at earlier stages. However, this segment gradually moved caudad, finally becoming horizontal to the body axis around CS 19, which was later by 4 stages than previously reported (Kim et al., 2003). The event seemed to be a result of the gradual movement of points S and E. Previous studies have reported the colorectum to be important for rotation (Frazer and Robbins, 1915; Dott, 1923), stating that as it becomes considerably elongated and rotates counterclockwise, it pushes the rest of the intestinal tract with it. However, movement of point E was not conspicuous in the present study; indeed, the position of point E relative to the origin was very stable, and what movement there was caudad. We observed the elongation of segment CE to be relatively slow, with the colorectum not playing a prominent role in the observed events.

On the other hand, the position of S to the origin, expressed by ∠s, changed dramatically during development, rotating nearly 180° during PUH, and the rate of elongation of the duodenum was similar to that of the increase in CRL. The movement of point S was caudad, almost along the medial plane. These findings suggest the movement of the start of the IL may be appropriately explained as the result of differential growth rather than rotation around the SMA.

The distance between S and E was almost constant. Maximal abdominal

transverse length increased by only 2.6 times from CS 16 to CS 23, so the final ratio of distance between S and E to abdominal transverse length was rather small. Point S was located almost in the median plane at CS 20, though the time at which it reached this position was earlier than previously described (Mall, 1898; Frazer and Robbins, 1915; Snyder and Chaffin, 1954; Dott, 1923; Kluth et al., 1995, 2003; Metzger et al., 2011).

Kluth et al. (1995, 2003) and Metzger et al. (2011) recently made detailed observations of midgut morphogenesis, including PUH and the process of return, in rats between embryonic days (EDs) 13 and 17. Six of their findings were consistent with ours. First, at ED 14 (corresponding to CS 18), the cecum was located to the left of the SMA as the result of the elongation of the small intestine in the umbilicus. Second, when the intestine entered the umbilical cord at ED 15 (corresponding to CS 20), the tip of the duodenojejunal area was already located beneath the root of the mesentery. Third, at ED 15, the position of the cecum varied between embryos. Fourth, at ED 15, the colorectum was mainly located in the abdominal coelom. Fifth, the active contribution of the colorectum to the development of the IL was small throughout the observation period. Sixth, the elongation rate differed by region and was not uniform. One notable difference was that the elongation of the duodenum was considerable in their study but relatively inconspicuous in ours.

Kluth et al. (1995, 2003) and Metzger et al. (2011) pointed out the formation of the duodenal loop, with rapid longitudinal elongation in the early phase and location beneath the root of the mesentery, as a distinct embryological process. Snyder and Chaffin (1954) consider the position of the

duodenum important because abnormal rotation of the IL tends to be accompanied by an abnormally positioned duodenum; however, Frazer and Robbins (1915) regard it as not important. For our part, we agree with Kluth et al. and Snyder and Chaffin that the early-stage positioning of the duodenojejunal loop beneath the root of the mesentery is a crucial factor which is related to the position of point S, though it may result not from the active elongation of the duodenum but rather from differential growth.

S and E were defined as the most obvious dorsal inflection points on the 3D image in the present study. In Soffer et al.'s study (2015), using a lateral view of a 3D reconstruction, two inflections concomitant with the change in length of the mesentery were clearly observed at points corresponding to S and E in our study. The point of inflection on the anal side was consistent with the boundary of blood supply between the SMA and inferior mesenteric artery, whereas the point on the oral side was located within the blood supply of the SMA. Thus, Soffers et al. regard the duodenum and proximal jejunum, including the inflection points, as part of the midgut loop, namely the first of four secondary loops of the midgut loop. The first secondary loop (proximal duodeno-jejunal loop) differed from other three loops in that the mesentery was thin at the oral side of the inflection, the elongation speed was not so rapid, and no tertiary loop was formed in that region; further, it was rotated 180 degrees relative to the SMA. These observations were almost consistent with ours, though the region was observed as part of segment PS (duodenum) in our study.

The morphology of the IL was rather simple until CS 18. O'Rahilly and Müller (1987) described the IL as entering the umbilical cord without coiling, a

317 finding similar to that of our present study. However, after CS 19, the small
318 intestinal portion (segment SC) elongated and formed a highly complex coiled,
319 spiral structure. To describe these movements precisely requires definitions of
320 the observation points and reference landmarks. Many previous studies have
321 not used such definitions, resulting in discrepancies among their descriptions of
322 rotation (Mall, 1898; Frazer and Robbins, 1915; O'Rahilly and Muller, 2001; Cyr
323 et al., 1986; Snyder and Chaffin, 1954; Kim et al., 2003; Dott, 1923; Kluth et al.,
324 1995, 2003; Metzger et al., 2011). The present study defined the observation
325 plane and origin by the proximal part of SMA, leading to clear and reliable
326 observations of the movement of points S and E. On the other hand, the
327 observed position of the cecum in the umbilical cord was still variable. One
328 obvious reason for this was that our observation plane was not defined with
329 reference to the cecum. To analyze the movement of the cecum, it would be
330 best to select an observation plane including the cecum itself; however,
331 anatomical reference points outside the intestinal tract, such as the SMA,
332 umbilical vein and arteries, mesentery, and omphaloenteric duct, will be
333 necessary.

334 The morphogenesis of looping of the embryonic gut and other tubular
335 organs such as the heart have recently been analyzed from a biophysical point
336 of view using biomechanical and computational models. Savin et al. (2011)
337 showed that the morphogenesis of intestinal looping is driven by the
338 homogeneous and isotropic forces that arise from differences in growth rates
339 between the intestine and the anchoring dorsal mesenteries. Hirashima (2014)
340 showed that axial tubular buckling triggered by cell proliferation drives the

morphogenesis of murine epididymal tubules through mechanical interactions between the developing epithelial tubule and its surrounding tissues. Bayraktar and Maenner (2014) indicate that cardiac looping may be driven by compressive loads resulting from unequal growth of the heart and pericardial cavity. Soffers et al. (2015) presented models explaining midgut looping, suggesting that the primary, secondary, and tertiary loops arise in hierarchical fashion; the primary and secondary loops may be regulated genetically, whereas the tertiary loops are variable, with their morphogenesis likely dependent on biophysical factors.

Our results indicate that rotation is a passive event both at earlier stages (CS 14–16) and at later stages (after CS17) (Fig. 7). The movement of segment SE may be explained as differential growth rather than rotation around the origin (SMA). The early-stage positioning of the duodenojejunal loop beneath the root of the mesentery is a crucial factor, though it may also result not from the active elongation of the duodenum. The morphogenesis of the intestinal tract continues after PUH, including events such as the return of the IL and cecum to the abdominal coelom and the fixation of each region in its appropriate final position. To fully determine the nature of IL rotation and its significance to the morphogenesis of the intestinal tract, future studies should observe IL development up to the end of fixation.

Acknowledgements

This study was supported by grants from the Japan Society for the Promotion of Science and the BIRD at the Japan Science and Technology

Agency (grant numbers #22591199, #24119002, #24790195, #25461642, #26220004, #15H01119, #15K15014, #15K08134). The authors thank Dr. Kohei Shiota, President of Shiga University of Medical Science, for providing the invaluable MR data. There are no conflicts of interest to be disclosed.

Literature cited

Bayraktar M, Maenner J. 2014. Cardiac looping may be driven by compressive loads resulting from unequal growth of the heart and pericardial cavity. Observations on a physical model. Front Physiol 5:1-15.

Cyr DR, Mack LA, Schoenecker SA, Patten RM, Shepard TH, Shuman WP, Moss AA. 1986. Bowel migration in the normal fetus: US detection. Radiology 161:119-121.

Dott NM. 1923. Anomalies of intestinal rotation: their embryological and surgical aspects, with report of five cases. Br J Surg 53: 251–286.

Frazer JE, Robbins RH. 1915. On the factors concerned in causing rotation of the intestine in man. J Anat Physiol 50: 75–110.

Hirashima T. 2014. Pattern formation of an epithelial tubule by mechanical instability during epididymal development. Cell Reports 9:866-873.

Kaigai N, Nako A, Yamada S, Uwabe C, Kose K, Takakuwa T. 2014. Morphogenesis and three-dimensional movement of the stomach during the human embryonic period. Anat Rec (Hoboken) 297: 791–797.

Kim WK, Kim H, Ahn DH, Kim MH, Park HW. 2003. Timetable for intestinal rotation in staged human embryos and fetuses. Birth Defects Res A Clin Mol Teratol 67:941-945.

Kluth D, Jaeschke-Melli S, Fiegel H. 2003. The embryology of gut rotation. Semin Pediatr Surg 12:275-279.

Kluth D, Kaestner M, Tibboel D, Lambrecht W. 1995. Rotation of the gut: fact or fantasy? J Pediatr Surg 30:448-453.

393 Mall FP. 1898. Development of the human intestine and its position in the adult.
394 Bull Johns Hopkins Hosp 9: 197–208.
395 Matsuda Y, Ono S, Otake Y, Handa S, Kose K, Haishi T, Yamada S, Uwabe C,
396 Shiota K. 2007. Imaging of a large collection of human embryo using a
397 super-parallel MR microscope. Magn Reson Med Sci 6:139-146.
398 Matsuda Y, Utsuzawa S, Kurimoto T, Haishi T, Yamazaki Y, Kose K, Anno I,
399 Marutani M. 2003. Super-parallel MR microscope. Magn Reson Med
400 50:183-189.
401 Meckel JF. 1817. Blindungsgeschichte des Darmkanals der Saugetiere und
402 namentlich der Menschen. Deutsche Arch Physiol 3: 1–84.
403 Metzger R, Metzger U, Fiegel HC, Kluth D. 2011. Embryology of the midgut.
404 Semin Pediatr Surg 20:145-151.
405 Nishimura H, Takano K, Tanimura T, Yasuda M. 1968. Normal and abnormal
406 development of human embryos: first report of the analysis of 1,213 intact
407 embryos. Teratology 1:281-290.
408 O'Rahilly R, Müller F. 1987. Developmental stages in human embryos : including
409 a revision of Streeter's Horizons and a survey of the Carnegie Collection.
410 Washington, D.C.: Carnegie Institution of Washington.
411 O'Rahilly R, Müller F. 2001. Human embryology and teratology. 3rd ed, New
412 York: Wiley-Liss.
413 Pernkopf E. 1925. Die Entwicklung der Form des Magendarmkanales beim
414 Menschen. II. Teil. 1. Abschnitt. Zschr f Anat Entwickl Gesch 77:1-143.
415 Savin T, Kurpios NA, Shyer AE, Florescu P, Liang H, Mahadevan L, Tabin CJ.
416 2011. On the growth and form of the gut. Nature 476:57-62.

Shiota K, Yamada S, Nakatsu-Komatsu T, Uwabe C, Kose K, Matsuda Y, Haishi T, Mizuta S, Matsuda T. 2007. Visualization of human prenatal development by magnetic resonance imaging (MRI). Am J Med Genet A 143A:3121-3126.

Snyder WH Jr, Chaffin L. 1952. An intermediate stage in the return of the intestines from the umbilical cord; embryo 37 mm. Anat Rec 113: 451–457.

Snyder WH Jr, Chaffin L. 1954. Embryology and pathology of the intestinal tract: presentation of forty cases of malrotation. Ann Surg 110: 368–380.

Soffers JH, Hikspoors JP, Mekonen HK, Koehler SE, Lamers WH. 2015. The growth pattern of the human intestine and its mesentery. BMC Dev Biol 15:31.

Yamada S, Uwabe C, Nakatsu-Komatsu T, Minekura Y, Iwakura M, Motoki T, Nishimiya K, Iiyama M, Kakusho K, Minoh M, Mizuta S, Matsuda T, Matsuda Y, Haishi T, Kose K, Fujii S, Shiota K. 2006. Graphic and movie illustrations of human prenatal development and their application to embryological education based on the human embryo specimens in the Kyoto collection. Dev Dyn 235:468-477.

Figure legends

Figure 1. The reference axis and anatomical landmarks used in the present study. (a) Illustration showing the reference axis and anatomical landmarks on the intestinal loop. The red broken line represents the border between the abdominal coelom and extraembryonic coelom in the umbilical cord, and the blue broken line connects the two reference points on the superior mesenteric artery (SMA), Z1 and Z2, which were used to define the z-axis and origin. P is the point located above the neural tube and vertebral column near the pyloric antrum, which was used to determine the median plane and y-axis. St is the stomach. (b) Reconstructed intestinal tract with anatomical references and 3D orthogonal coordinate system. (c) Measure for height of the PUH. (d) Orthogonal coordinate system. The SMA is the origin. P, pyloric antrum; S, start of intestinal loop; E, end of intestinal loop; C, cecum; T, tip of the intestinal loop; B, area on the colon crossing the border between the abdominal coelom and extraembryonic coelom; ∠Ro, angle between median plane and segment SE; ∠s, angle between S and median plane; ∠e, angle between E and median plane

Figure 2. Representative 3D reconstructions of intestinal tract between CS 14 and CS 23. (a) Ventral views (CS 14, 15). (b) Representative images at CS 16: mid-sagittal section of MR image (i), lateral view with silhouette of embryo (ii), and ventral (iii) and lateral (iv) views of a reconstruction of the intestinal tract alone. (c) Representative images at CS 18: mid-sagittal section of MR image (i);

lateral (ii) and ventral (iii) views with silhouette of embryo. The afferent part of the intestinal loop runs on the right of the SMA, with the efferent part and cecum on the left. The SMA runs parallel to the straight parts of the intestinal loop. (d) Lateral view of embryos between CS 19 and CS 23.
St, stomach; C, cecum, Va, vermiform appendix; Oe, omphaloenteric duct; red broken line, border between abdominal coelom and extraembryonic coelom in umbilical cord; white line, z-axis. T = height of the PUH (mm); scale bar = 1 mm

Figure 3. Elongation of intestinal tract between CS 14 and CS 23. The crown-rump length (CRL) is indicated in line graphs for comparison. Data for regional growth are provided only for CS 16 onward, because points C and S were not evident at CS 14.

Figure 4. Changes in height of the intestinal tract between CS 14 and CS 23, indicating the degree of PUH. The crown-rump length (CRL) and height of the border between the abdominal coelom and the extraembryonic coelom in the umbilical cord are indicated as broken lines for comparison.

Figure 5. Movement of the anatomical landmarks: points S and E (a) and point C (b). The line following the straight portion of the SMA was defined as the z-axis. The points were projected to the xy plane near the proximal part of the SMA, corresponding to the dorsal wall of the abdominal coelom.

Figure 6. Relationships of points S and E with the origin (SMA). The angles from each anatomical landmark to the median plane were plotted during development. ∠Ro, angle between median plane and segment SE; ∠s, angle between S and median plane; ∠e, angle between E and median plane.

Figure 7. Illustrations showing the movement (viewed ventrally) of the start (S) and end (E) of the intestinal loop and their positions in relation to the proximal part of the SMA, designated as the origin (O). (a) Before rotation. (b) Expected movement according to the classical en bloc model of 90-degree counterclockwise rotation around SMA as origin. (c) Movement observed between CS 14 and CS 16. (d) Movement observed from CS 14 to CS 23 (end of PUH stage).

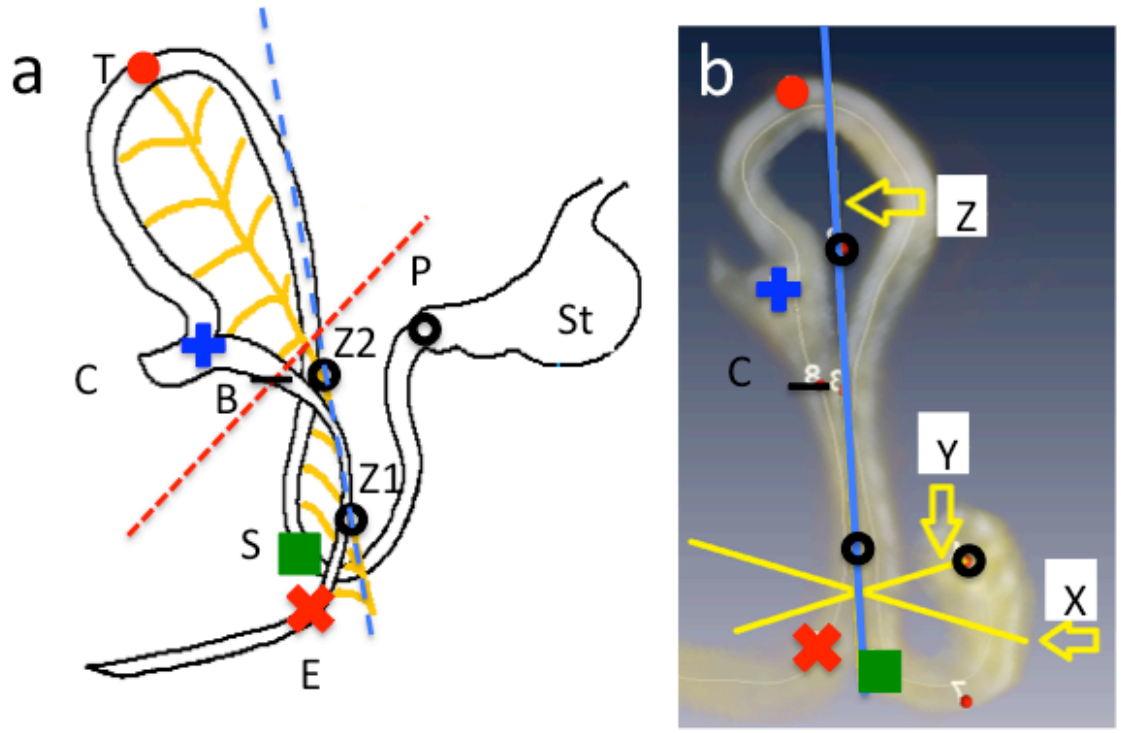
a
T
P
St
Z2
C
B
Z1
S
E
b
Z
C
Y
X
c
T
C
B
d
∠s
O (SMA)
∠e
S
∠Ro
E

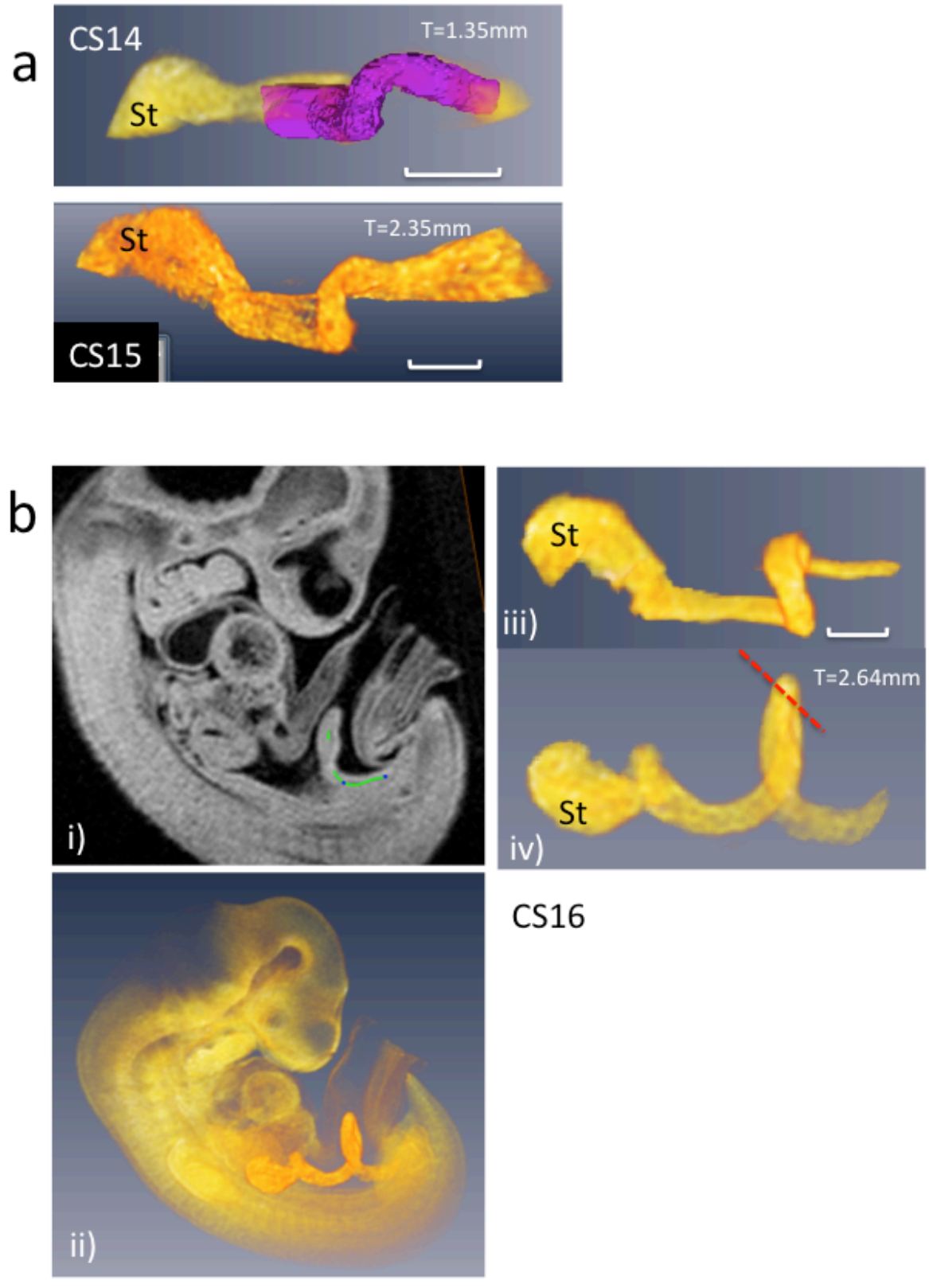
a
CS14
T=1.35mm
St
St
T=2.35mm
CS15
b
i)
iii)
St
T=2.64mm
St
iv)
ii)
CS16

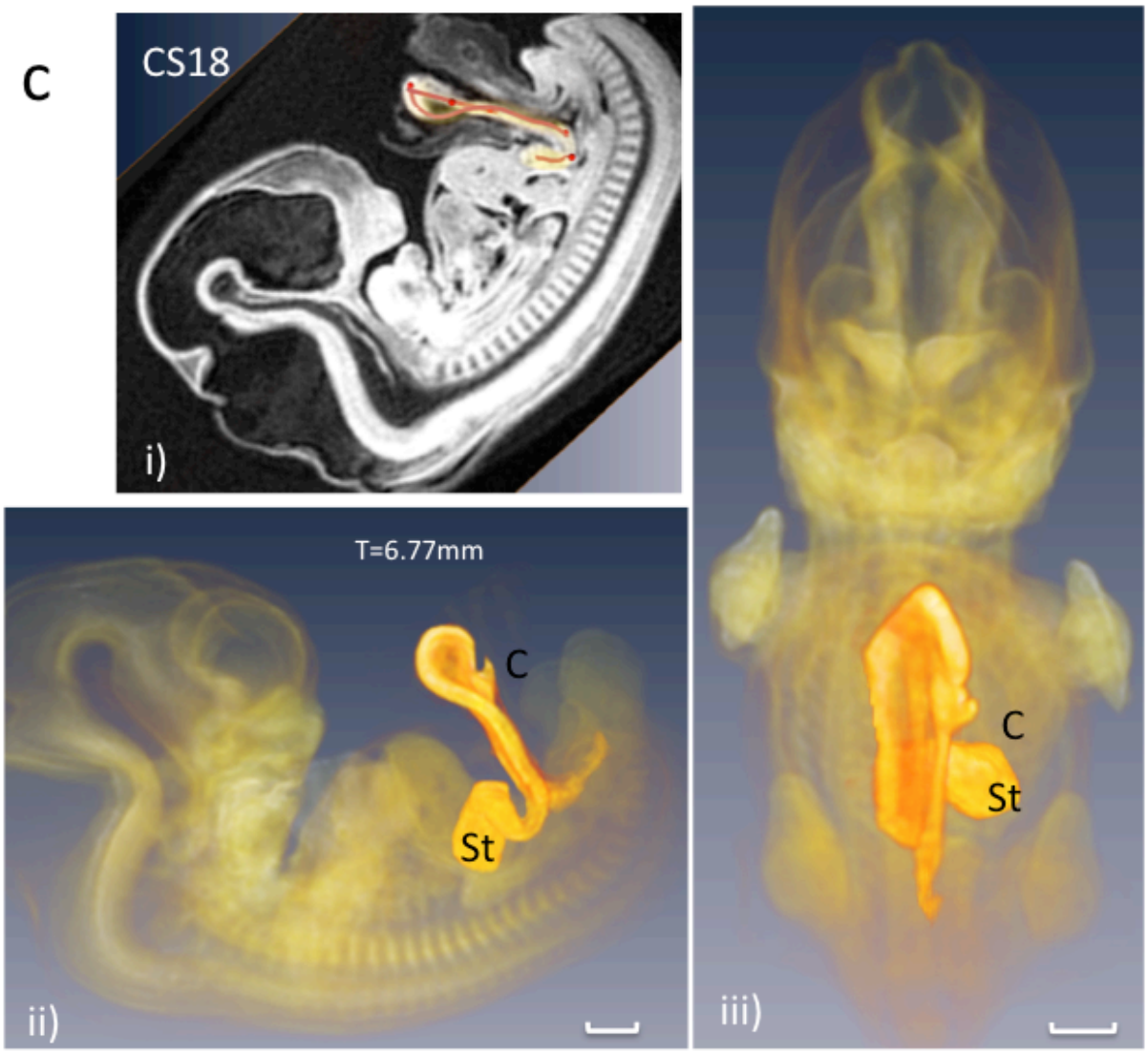
C
CS18
i)
T=6.77mm
C
St
ii)
C
St
iii)

d

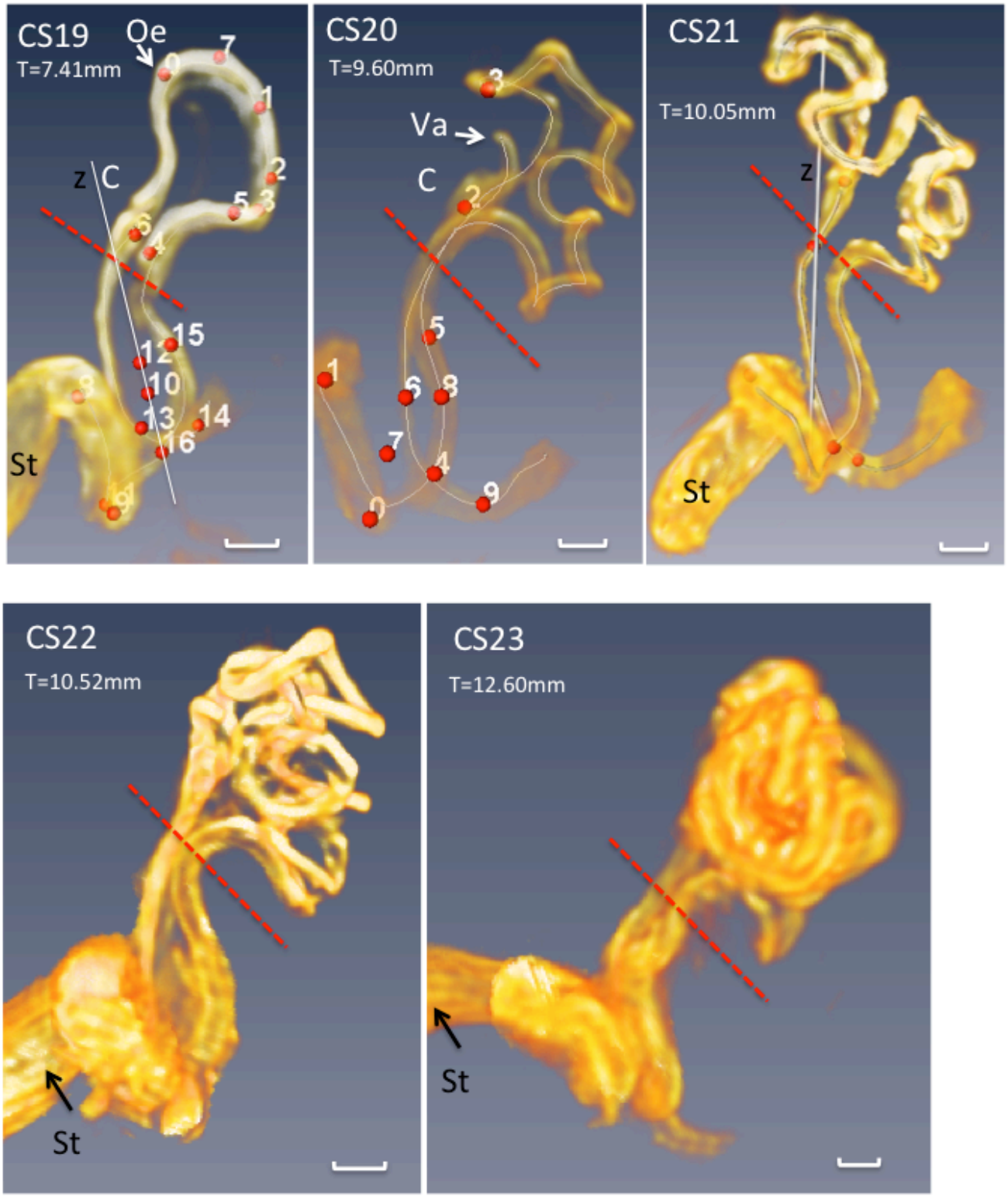
CS19
T=7.41mm
Oe
z
C
St
CS20
T=9.60mm
Va
C
CS21
T=10.05mm
z
St
CS22
T=10.52mm
St
CS23
T=12.60mm
St

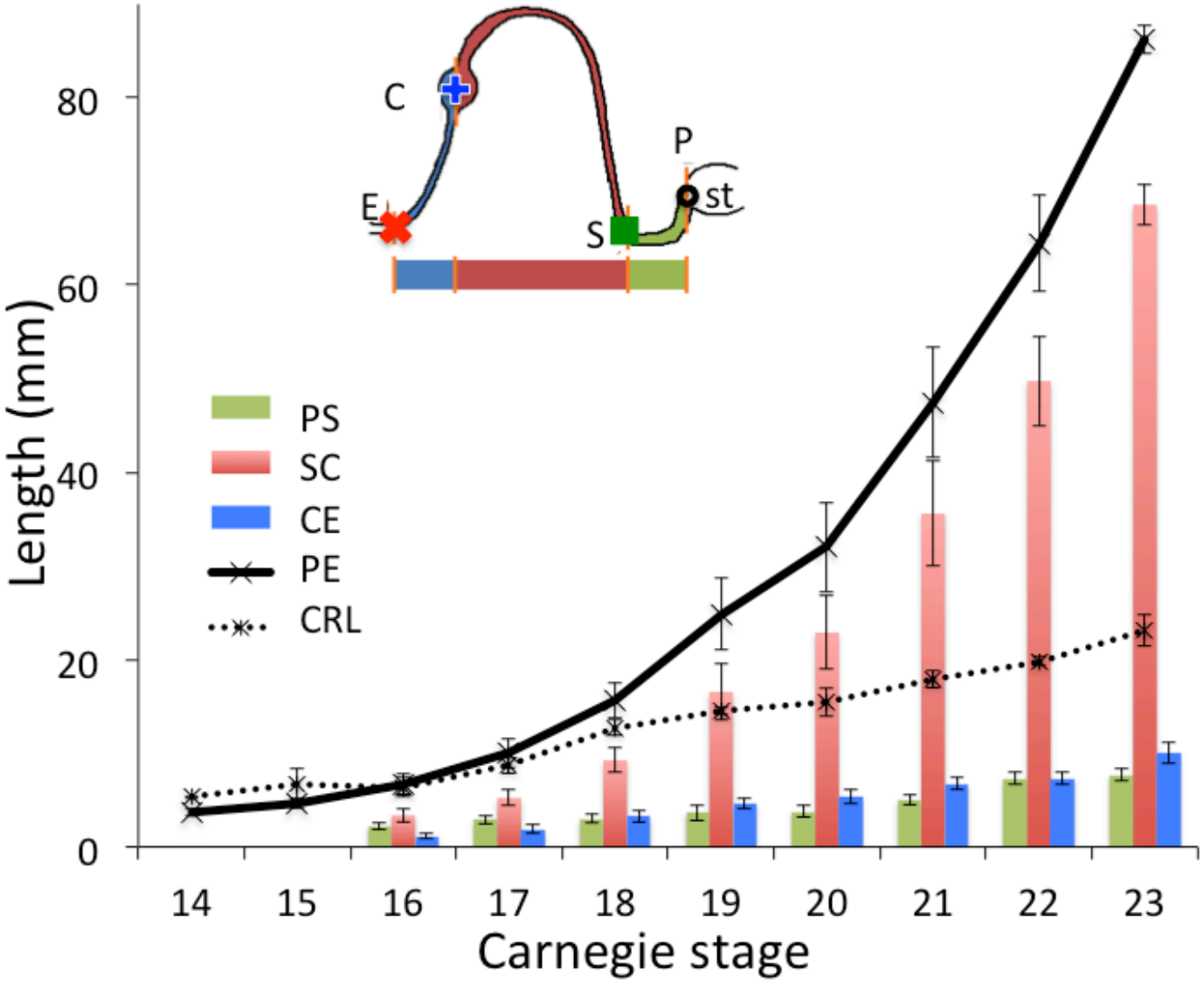
Length (mm)
0
20
40
60
80
14
15
16
17
18
19
20
21
22
23
Carnegie stage
PS
SC
CE
PE
CRL
C
E
S
P
st

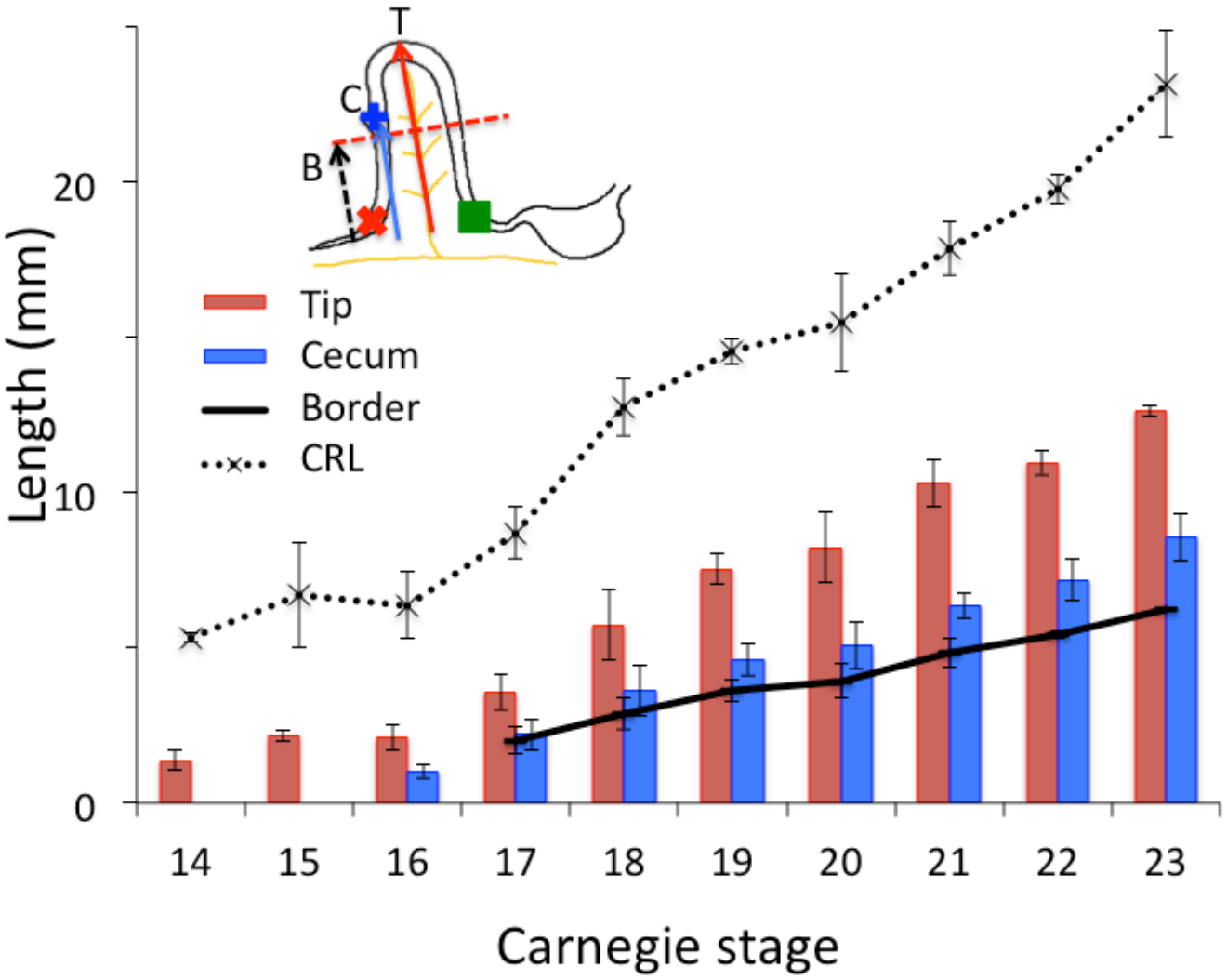
T
C
B
Tip
Cecum
Border
CRL
Length (mm)
0
10
20
14
15
16
17
18
19
20
21
22
23
Carnegie stage

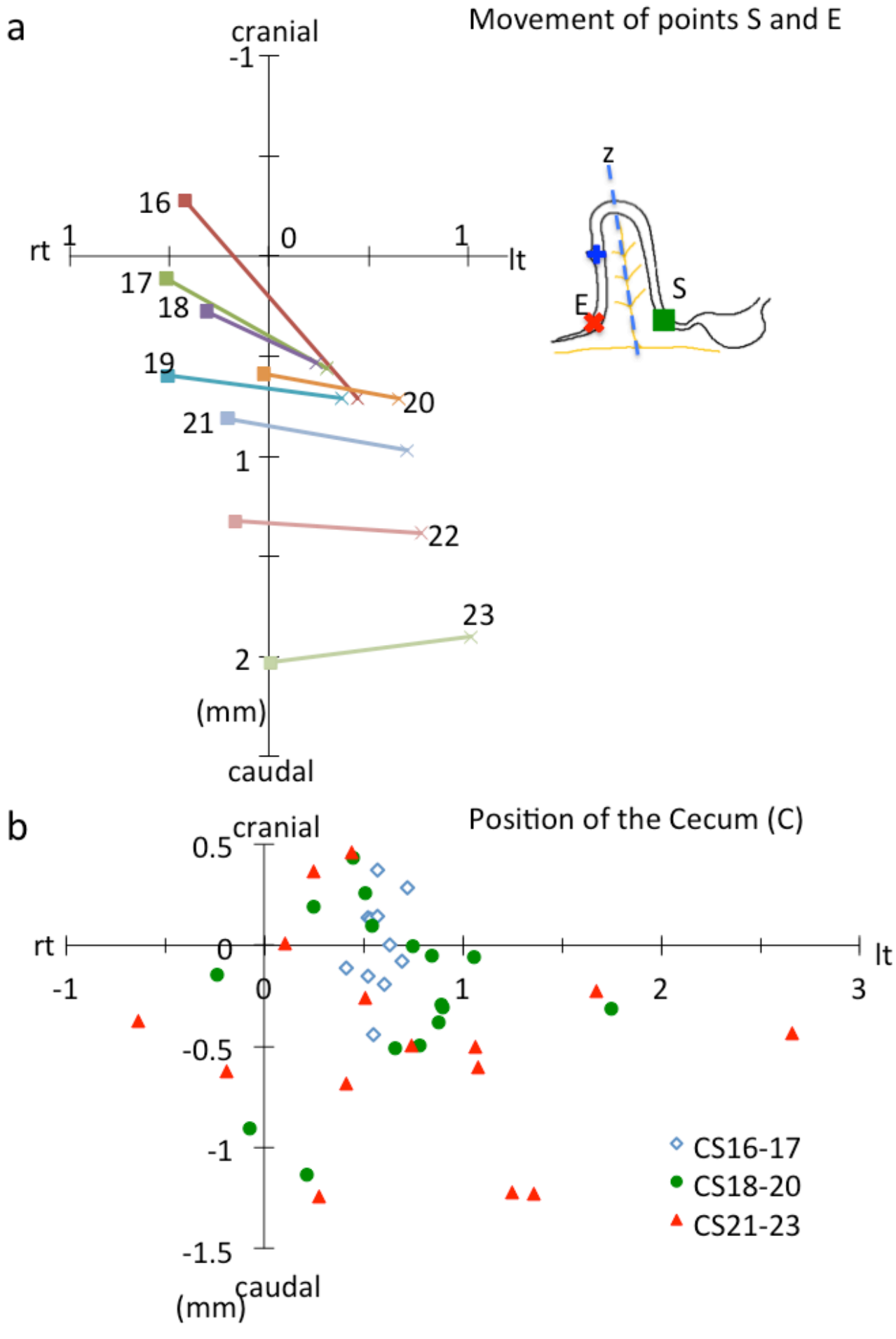
a
Movement of points S and E
cranial
-1
rt
1
0
1
lt
16
17
18
19
20
21
22
23
1
2
(mm)
caudal
z
E
S
b
Position of the Cecum (C)
cranial
0.5
rt
0
lt
-1
0
1
2
3
-0.5
-1
-1.5
caudal
(mm)
CS16-17
CS18-20
CS21-23

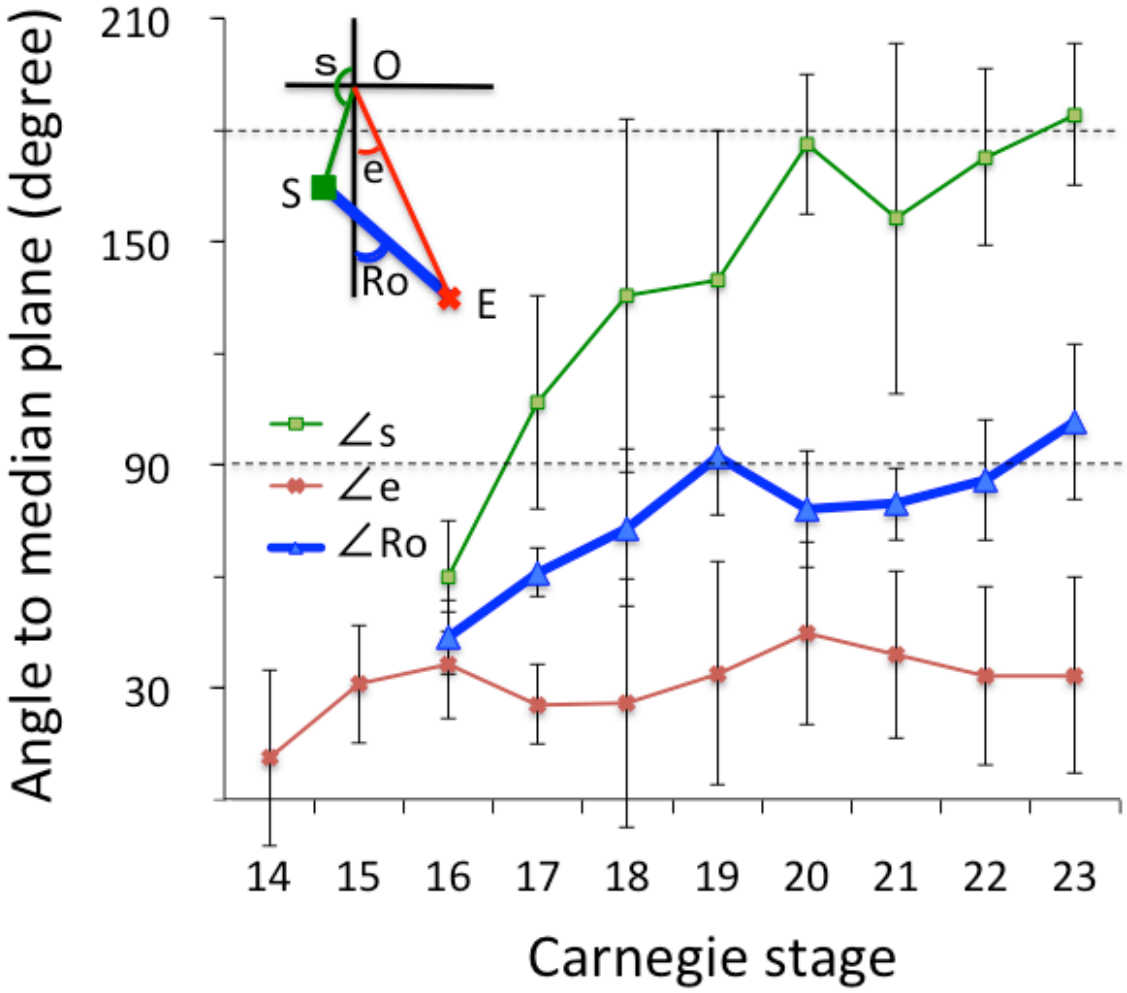
Angle to median plane (degree)
210
150
90
30
s
O
e
S
Ro
E
∠s
∠e
∠Ro
14
15
16
17
18
19
20
21
22
23
Carnegie stage

a

b

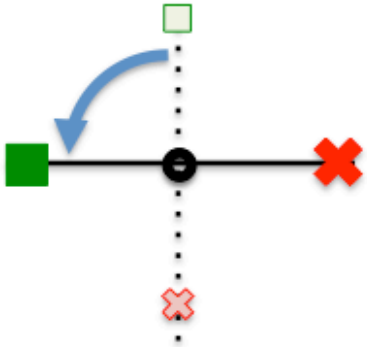

c

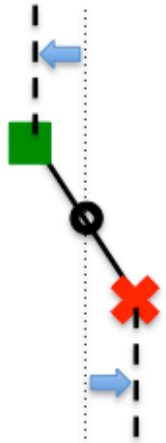

d